Corrosion Protective Bi-Layered Composites of Polyaniline and Poly(*o*-anisidine) on Low Carbon Steel

Sudeshna Chaudhari, P. P. Patil

Department of Physics, North Maharashtra University, Jalgaon 425 001, Maharashtra, India

Received 23 October 2007; accepted 21 January 2008
DOI 10.1002/app.28367
Published online 9 May 2008 in Wiley InterScience (www.interscience.wiley.com).

ABSTRACT: Bi-layered composites of polyaniline (PANI) and poly(*o*-anisidine) (POA) were investigated for corrosion protection of low carbon steel (LCS). In this work, homopolymers and bi-layers of PANI and POA were electropolymerized on LCS from an aqueous salicylate solution by using cyclic voltammetry. These coatings were characterized by cyclic voltammetry, Fourier transform infrared (FTIR) spectroscopy and scanning electron microscopy (SEM). Corrosion tests were carried out in aqueous 3% NaCl solution for LCS coated with PANI, POA, bi-layered POA/PANI (POA on top of the PANI) or PANI/POA (PANI on top of the POA) composites using open circuit potential (OCP) measurements, potentiodynamic polarization technique, and electrochemical impedance spectroscopy (EIS). The single layer of PANI and POA protected the LCS in 3% NaCl for 8 and 16 h, respectively. The bi-layered composite coatings provide effective protection to LCS for a longer time than a single layered PANI or POA coating. However, the corrosion protection offered to LCS depends on the deposition order of polymer layers in the composite. The PANI/POA composite provides better protection to LCS against corrosion than POA/PANI coating. © 2008 Wiley Periodicals, Inc. J Appl Polym Sci 109: 2546–2561, 2008

Key words: corrosion protective coatings; conducting polymersbilayers; polyaniline; poly(*o*-anisidine); cyclic voltammetry; low carbon steel; electrochemical impedance spectroscopy

INTRODUCTION

During last decade, electrically conducting polymers have been widely investigated as corrosion protective coatings, because they can be easily synthesized on metallic surfaces from aqueous media by electrochemical polymerization route.[1–20] The main problem related to the electrochemical synthesis of conducting polymer coatings on oxidizable metals is dissolution of the base metal in the beginning of polymerization, so only few electrolytes suitable for polymerization were reported. The electrochemical synthesis of conducting polymer coatings from aqueous solutions containing oxalate ions has been investigated by several groups[9,20–23] because this medium inhibits iron dissolution. Other electrolytes such as salicylate,[18,24] tartrate,[25,26] malate,[27] and sulfate[10] have also been employed for the electrochemical synthesis of conducting polymers. The extent of using these conducting polymers is limited due to the exclusivity of the monomers that are essential for their synthesis. To overcome this limitation, different synthesis approaches have been attempted.

The first approach involves the use of copolymerization to prepare new polymers with inbuilt tailormade properties suitable for the application. We have reported recently, the synthesis of poly(aniline-*co*-*o*-toluidine) coatings on LCS from aqueous salicylate solution using cyclic voltammetry and investigated the corrosion properties of these copolymer coatings in aqueous 3% NaCl.[28] It was found that the poly(aniline-*co*-*o*-toluidine) coatings provide better protection for LCS against corrosion than corresponding homopolymer coatings. The corrosion rates of PANI, poly(*o*-toluidine) (POT) and poly(aniline-*co*-*o*-toluidine) (with feed ratio of *o*-toluidine as 0.5) coated LCS are found to be ~3, 20, and 50 times lower than that observed for uncoated LCS. Hur et al.[29] reported the electrochemical synthesis of poly(aniline-*co*-2-toluidine) films on stainless steel in tetrabutylammonium perchlorate/acetonitrile solution containing perchloric acid. They found that the PANI coatings provide much better protection to stainless steel than poly (2-anisidine) and poly(aniline-*co*-2-anisidine) films. It has been shown that the protection properties of PANI are related to the passivation of steel and barrier effect, while the protection of steel by poly(2-anisidine) and poly(aniline-*co*-2-anisidine) films is mainly

This article contains supplementary material available via the Internet at http://www.interscience.wiley.com/jpages/0021-8995/suppmat.

Correspondence to: P. Patil (pnmu@yahoo.co.in).

Contract grant sponsor: University Grants Commission (UGC), New Delhi, India.

through the barrier effect. Bereket et al.[30] synthesized poly(aniline-*co*-2-anisidine) films on stainless steel by using the synthesis conditions identical to those used by Hur et al.[29] They found that the PANI, poly (2-anisidine) and poly(aniline-*co*-2-anisidine) films have corrosion protection effect for stainless steel in aggressive medium of 0.5 HCl solution. However, the durability of the poly(aniline-2-anisidine) films is limited to 3 h. More recently, we synthesized poly(*o*-anisidine-*co*-*o*-toluidine) coatings on Cu from aqueous salicylate solution and investigated the corrosion properties of these copolymer coatings in aqueous 3% NaCl.[31] The corrosion rates of POA, POT and poly (*o*-anisidine-*co*-*o*-toluidine) (with feed ratio of *o*-toluidine as 0.5) coated Cu are found to be ~9, 27, and 720 times lower than that observed for uncoated Cu.

The second approach involves the formation of bilayer coatings which either consists of a top coat of conducting polymer on the layer of the other conducting polymer or a top layer of conducting polymer on the metallic coating such as nickel. Yagan et al.[32] electropolymerized the single layers and bilayers of PANI and polypyrrole (PPY) on mild steel in aqueous oxalic acid solution and investigated their corrosion behavior in aqueous 0.5*M* NaCl and 0.1*M* HCl solutions. Unexpectedly, the bilayers of PANI and PPY did not provide better protection for mild steel against corrosion than corresponding single layer coatings. On contrary, the single layered PPY coating exhibited the best corrosion resistance among all coatings. Tuken and his research group[33–36] extensively studied the electrochemical synthesis of PANI and PPY coatings on nickel plated mild steel and Cu substrates from aqueous media.

The third approach involves the synthesis of hybrid composite coatings of conducting polymer and one or more environmentally friendly oxides. More recently, we have synthesized the poly(*o*-toluidine)/ZrO_2 nanocomposite coatings on mild steel in ZrO_2-containing aqueous tartrate solution by using cyclic voltammetry.[37] It was observed that the poly(*o*-toluidine)/ZrO_2 nanocomposite coating provides better protection to mild steel against corrosion in aqueous 3% NaCl with respect to poly(*o*-toluidine). The composite coating reduced the corrosion rate of mild steel almost by a factor of 51.

In this article, we present the first evaluation of corrosion protection effect in aqueous 3% NaCl for the bi-layered composites of PANI and POA on LCS in comparison with that of the single layers of PANI and POA by using OCP measurements, potentiodynamic polarization technique and EIS. The single layers and bi-layered composites of PANI and POA were synthesized on LCS substrates from aqueous salicylate medium and characterized by cyclic voltammetry, FTIR, and SEM.

EXPERIMENTAL

Materials

All chemicals were of analytical grade. The monomers, aniline and *o*-anisidine were procured from Fluka and were doubly distilled prior to being used for the synthesis. Sodium salicylate ($NaC_7H_5O_3$) was procured from Merck and used as-received without further purification. Bi-distilled water was used to prepare all the solutions.

Substrate preparation

The chemical composition (by weight %) of LCS used in this study was : 0.03% C, 0.026% S, 0.01% P, 0.002% Si, 0.04% Ni, 0.002% Mo, 0.16% Mn, 0.093% Cu, and 99.64% Fe. The LCS substrates (size ~ 10 × 15 mm and 0.5-mm thick) were polished with a series of emery papers, followed by thorough rinsing in acetone and double distilled water and dried in air. Prior to any experiment, the substrates were treated as described and freshly used with no further storage.

Electrochemical syntheses

The electrochemical syntheses were carried out under cyclic voltammetric conditions in a single compartment three electrode cell with LCS as working electrode (150 mm^2), platinum as counter electrode and saturated calomel electrode (SCE) as reference electrode. The cyclic voltammetric conditions were maintained using the electrochemical measurement System (SI 1280B, Solartron, UK) controlled by corrosion software (CorrWare, Electrochemistry/Corrosion Software, Scribner Associates, supplied by Solartron, UK).[38] The schematic representation of bi-layered composites of PANI and POA synthesized on LCS is shown in Figure 1. These bi-layered composites were synthesized on LCS using the following procedures.

POA/PANI coatings (bi-layered composite-POA on the top of the PANI)

The PANI film was first synthesized on LCS substrate in 0.1*M* aqueous salicylate solution containing 0.3*M* aniline by using cyclic voltammetry. Thereafter, POA layer was deposited over the PANI film from 0.1*M* aqueous salicylate solution containing 0.1*M* *o*-anisidine to prepare a POA/PANI bi-layered coating. Both layers were synthesized by cycling the electrode potential between −1.0 and 1.8 V with the scan rate of 0.02 V/s. After deposition, the working electrode was removed from the electrolyte and rinsed with double distilled water and dried in air.

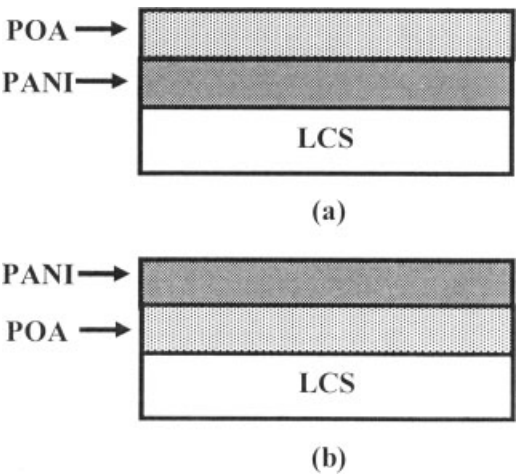

Figure 1 Schematic representation of bi-layered composites synthesized on LCS (a) POA/PANI and (b) PANI/POA.

Pani/POA coatings (bi-layered composite-PANI on the top of the POA)

The procedure and experimental conditions were identical to those for the POA/PANI bi-layered coating, except that the order in which the single layers were coated was reversed. Hence, the PANI film was deposited on top of the POA film.

Characterization

The FTIR transmission spectra were recorded with a Perkin–Elmer spectrometer (1600 Series II, USA) in horizontally attenuated total reflectance (HATR) mode in the spectral range 4000–400 cm^{-1}. SEM images were recorded with a Leica Cambridge 440 Microscope (Cambridge, England, UK). The thickness of the coatings was measured by a conventional magnetic induction based microprocessor controlled coating thickness gauge (Minitest 600, ElectroPhysik, Germany). The error in the thickness measurements was less than 5%.

Evaluation of corrosion protection performance

The corrosion protection performance of the coatings was evaluated in 3% NaCl solution by using open circuit potential (OCP) measurements, potentiodynamic polarization technique and EIS using a electrochemical measurement system (SI 1280B, Solartron, UK). For these measurements, a teflon holder was used to encase the polymer coated LCS substrates so as to leave an area of ~ 0.4 cm^2 exposed to the solution. All the measurements were repeated at least four times and good reproducibility of the results was observed.

The potentiodynamic polarization measurements were performed by sweeping the potential between -0.25 and 0.25 V from OCP with the scan rate of 0.002 V/s. The potentiodynamic polarization curves were analyzed by using Corr-view software from Scribner Associates which performs the Tafel fitting and calculates the values of the corrosion potential (E_{corr}), corrosion current density (j_{corr}) and corrosion rate (CR) in mm per year.

The Nyquist impedance plots were recorded at the OCP in the frequency range from 0.1 to 20 kHz with amplitude of superimposed AC signal of 0.010 V. The spectra were also recorded after different immersion times in aqueous 3% NaCl medium. The analysis of the impedance spectra was done by fitting the experimental results to equivalent circuits using Z-view software from Scribner Associates.[39] The quality of fitting to equivalent circuit was judged firstly by the chi-square value (χ^2, i.e., the sum of the square of the differences between theoretical and experimental points) and secondly by limiting the relative error in the value of each element in the equivalent circuit to 5%.

RESULTS AND DISCUSSION

Synthesis of single PANI and POA layers on LCS

PANI layer on LCS

The cyclic voltammograms recorded during the first, second, and tenth potential sweeps on an uncoated LCS electrode in an aqueous solution containing 0.3*M* aniline and 0.1*M* sodium salicylate are shown in Figure 2(a). These cyclic voltammograms exhibit good resemblance with those reported by Pawar et al.[40] and have some common features such as: (i) In the first potential sweep, the anodic (A_1) and corresponding cathodic (*C*) peaks at ~ 1.36 and -0.605 V versus SCE, respectively. The anodic peak A_1 corresponds to the oxidation of aniline and formation of radical cations, which is considered to be the first step in the polymerization of the conducting polymers. The cathodic peak C is attributed to the partial reduction of the anodically formed species on the LCS electrode. (ii) During second potential sweep, an increase in the current density is observed in the potential range ~ 0.048–0.737 V versus SCE and rest of the features are similar to that of the first sweep. An increased in the current density in the potential range 0.048–0.737 V is assigned to the oxidation of PANI deposited at the LCS surface[41] and (iii) In subsequent sweeps, the voltammograms identical to that of second sweep are obtained. However, the current density corresponding to the redox peaks increases gradually with an increase in the number of sweeps.

$$d = \frac{QM}{2F\rho} \quad (1)$$

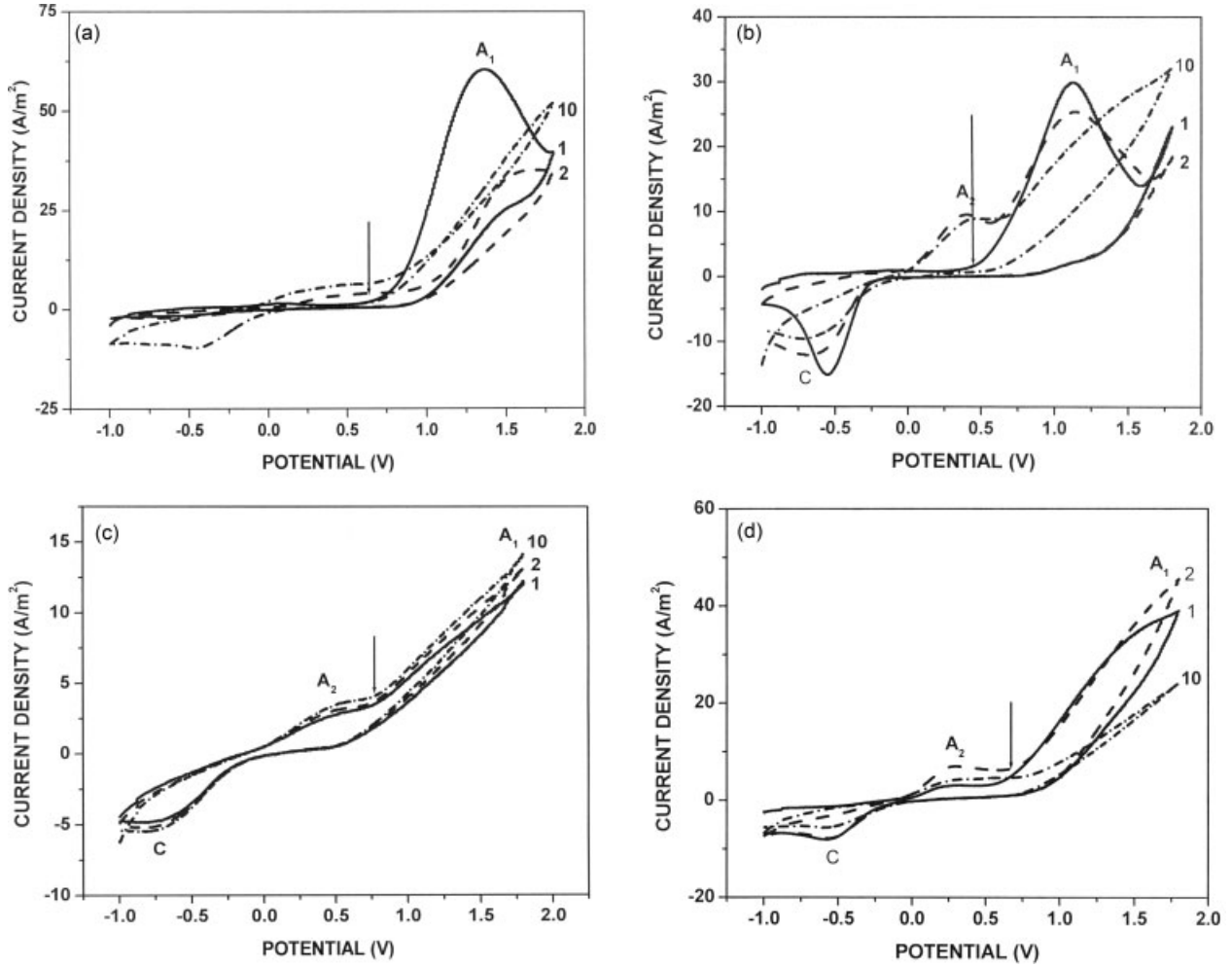

Figure 2 (a) Cyclic voltammograms recorded during the (1) first, (2) second and (10) tenth potential sweep on uncoated LCS electrode in an aqueous solution containing 0.3*M* aniline and 0.1*M* sodium salicylate. (b) Cyclic voltammograms recorded during the (1) first, (2) second and (10) tenth potential sweep on uncoated LCS electrode in an aqueous solution containing 0.1*M* *o*-anisidine and 0.1*M* sodium salicylate. (c): Cyclic voltammograms recorded during the (1) first, (2) second and (10) tenth potential sweep of a PANI coated LCS in an aqueous solution containing 0.1*M* *o*-anisidine and 0.1*M* sodium salicylate. (d) Cyclic voltammograms recorded during the (1) first, (2) second, and (10) tenth potential sweep of a POA coated LCS in an aqueous solution containing 0.3*M* aniline and 0.1*M* sodium salicylate.

The coating thickness was also estimated by using the equation[42] assuming a two electron mechanism based on the monomer involved in the polymerization process and a current efficiency of 100%. In this equation, Q is the specific overall charge for the electrochemical polymerization, ρ is the density of the PANI and M is the molar mass and F is the Faraday constant. The thickness of PANI layer (20 sweeps) calculated by using this equation was found to be $\sim$ 2.9 μm [standard deviation (SD) = 0.085], which is in fairly agreement with that measured by using a conventional magnetic induction based microprocessor controlled coating thickness gauge.

The FTIR spectrum of PANI coating synthesized on LCS recorded in HATR mode is shown in Figure 3(a). Main characteristic bands of PANI are assigned as follows.[43–46] A broad band at $\sim$ 3367 cm^{-1} is due to the *N*—H stretching mode, the C=N and C=C stretching mode for the quinoid (Q) and benzoid (B) rings occur at 1656 and 1448 cm^{-1} respectively, a band at $\sim$ 1379 cm^{-1} is assigned to the C—N stretching, the bands at $\sim$ 1774 and 1277 cm^{-1} is assigned to the presence of carboxylic groups of sodium salicylate, the bands at 1126 and 1071 cm^{-1} are attributed to the 1–4 substitution on the benzene ring and the bands between 800 and 700 cm^{-1} reveal the occurrence of the 1–3 substitutions.

POA layer on LCS

The cyclic voltammograms recorded during the first, second, and tenth potential sweeps on an uncoated LCS electrode in an aqueous solution containing 0.1*M* *o*-anisidine and 0.1*M* sodium salicylate are shown in Figure 2(b). These cyclic voltammograms exhibit good resemblance with those reported by Wankhede et al.[24] and have some common features

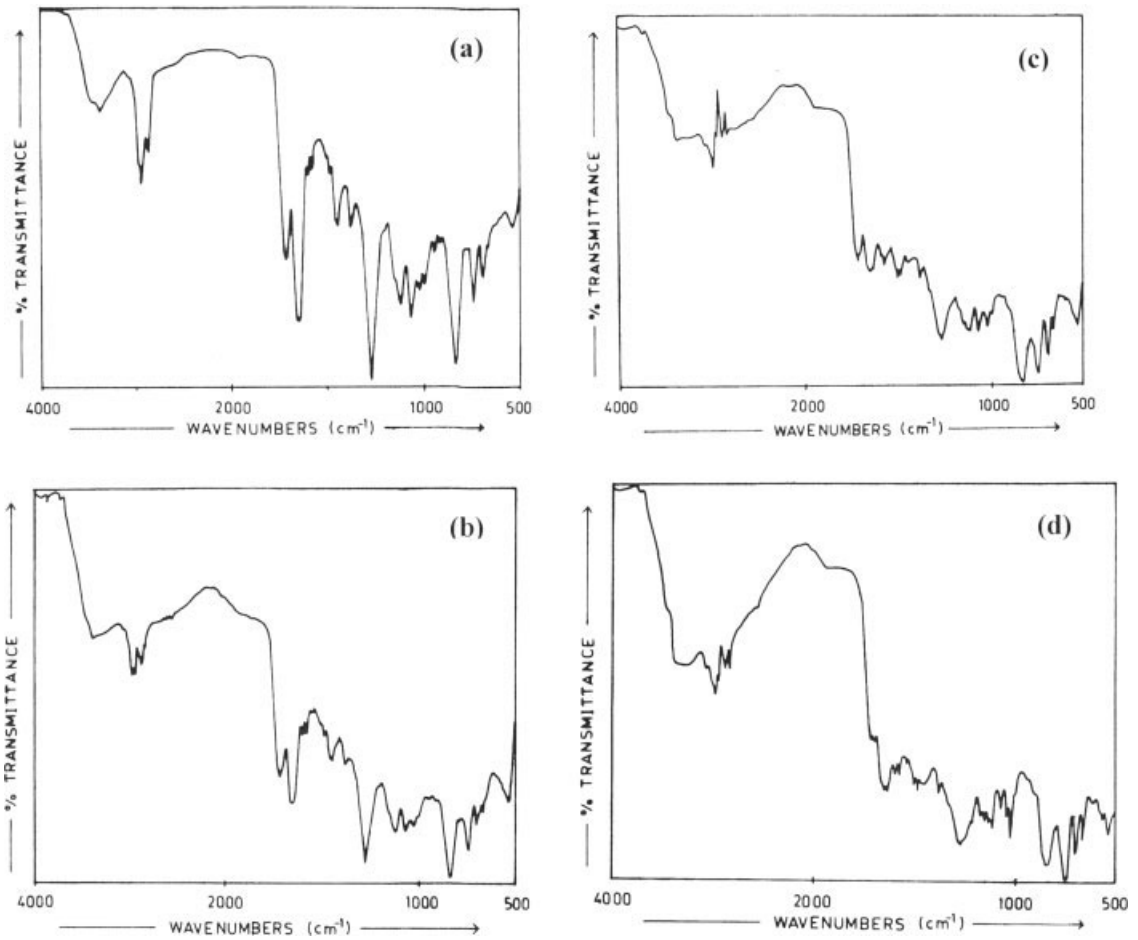

Figure 3 FTIR spectra of (a) PANI, (b) POA, (c) POA/PANI, and (d) PANI/POA coatings synthesized on LCS substrate.

such as: (i) In the first potential sweep is characterized by anodic (A_1) and corresponding cathodic (C) peaks at $\sim$ 1.132 and -0.551 V versus SCE, respectively. The anodic peak A_1 is attributed to oxidation of *o*-anisidine since a black, uniform film is generated on the steel substrate. The cathodic peak C corresponds to the partial reduction of the deposited POA film. (ii) During the second sweep, a new broad anodic peak A_2 observed at $\sim$ 0.372 V versus SCE is assigned to the oxidation of POA deposited at the steel surface, which corresponds to conversion of amine units into radical cations[41] and (iii) On repetitive sweeping, the voltammograms identical to that of second sweep are obtained. However, the current density corresponding to the anodic peaks increases gradually with the number of sweeps. After fourth sweep, the cyclic voltammogram does not show well-defined redox peaks. A typical tenth scan is also shown in Figure 2(b). The thickness of POA layer (20 sweeps) calculated by using the eq. (1) was found to be $\sim$ 6 μm (SD = 0.081).

The FTIR spectrum of the POA recorded in HATR mode [Fig. 3(b)] exhibits main characteristic bands of POA, which are assigned as follows.[43–46] A broad band at $\sim$3410 cm^{-1} is due to *N*—H stretching mode, the C=N and C=C stretching mode for the Q and B rings occur at 1655 and 1578 cm^{-1} respectively, the bands at $\sim$ 1716 and 1276 cm^{-1} are assigned to the presence of carboxylic groups of sodium salicylate, the bands at $\sim$ 1122 and 1071 cm^{-1} are attributed to the presence of an *o*-methoxy group, a band at 837 cm^{-1} indicates that *ortho* substituted benzene ring and the bands between 800 and 700 cm^{-1} reveal the occurrence of the 1–3 substitutions.

Synthesis of bi-layered composites of PANI and POA on LCS

Bi-layered POA/PANI composite on LCS

Figure 2(c) shows the cyclic voltammograms recorded during the first, second and tenth potential sweeps of a PANI coated LCS in an aqueous solution containing 0.1*M* *o*-anisidine and 0.1*M* sodium salicylate. Previously, the PANI layer was deposited on LCS by cycling the potential between -1.0 and 1.8 V versus SCE in an aqueous solution containing 0.3*M* aniline and 0.1*M* sodium salicylate at a scan rate of 0.02 V/s (10 cycles). In the first sweep, broad and small an-

odic, and corresponding cathodic peaks at ~ 0.455 and −0.734 V versus SCE, respectively, are observed. The onset of oxidation wave is observed at ~ 0.725 V versus SCE, which obviously corresponds to oxidation of *o*-anisidine. This cyclic voltammogram exhibits good resemblance with the tenth potential sweep [cf. Fig. 2(b)] recorded during the synthesis of POA layer on LCS electrode. However, the current densities corresponding to the redox peaks are markedly lower than one observed with an uncoated LCS electrode, indicating a lower rate of polymerization of *o*-anisidine on an electrode already covered with a PANI. This may be due to the partial blocking of the electrode surface by previously deposited PANI layer. It is believed that during the electrochemical polymerization, *o*-anisidine and the supporting electrolyte anions diffuse through the micropores in PANI towards the LCS surface. Subsequently, the polymerization begins within the micropores and expands over the entire electrode surface with increasing the number of potential sweeps. Thus, the rate of polymerization is expected to be appreciably slow due to the diffusion hindrance. In the first sweep, broad and small anodic and corresponding cathodic peaks at ~ 0.455 and −0.734 V versus SCE, respectively, are observed. The onset of oxidation wave is observed at ~ 0.725 V versus SCE, which obviously corresponds to oxidation of *o*-anisidine. It is clearly observed that the oxidation wave (indicated by an arrow) on PANI coated LCS is reduced by almost ~ 0.301 V versus SCE. This implies that the PANI layer formed on the LCS surface does not constitute a barrier to the electronic transfer. In subsequent sweeps, the voltammograms identical to that of first sweep are obtained. However, the current densities corresponding to the redox peaks are observed to increase with an increase in the number of sweeps, which substantiates the growth of the conducting polymer. This reveals the growth of the conducting POA layer on the PANI coated LCS, thereby indicating the formation of bi-layered POA/PANI composite on the LCS. The thickness of bi-layered POA/PANI composite calculated by using the eq. (1) was found to be ~ 6 μm (SD = 0.081).

The FTIR spectrum of POA/PANI coating on LCS recorded in HATR mode is shown in Figure 3(c). The most striking feature of this spectrum is that it exhibits very similar characteristics to those of POA. This indicates that the electrochemical polymerization of *o*-anisidine occurs on PANI layer and results into the formation of bi-layered POA/PANI composite on the LCS.

Bi-layered PANI/POA composite on LCS

The cyclic voltammograms recorded during the first, second and tenth sweeps of a POA coated LCS electrode in an aqueous solution containing 0.3*M* aniline and 0.1*M* sodium salicylate are shown in Figure 2(d). Initially, the POA layer was deposited on LCS by cycling the potential between −1.0 and 1.8 V versus SCE in an aqueous solution containing 0.1*M* *o*-anisidine and 0.1*M* sodium salicylate at a scan rate of 0.02 V/s (10 cycles). The first sweep exhibits—(i) a plateau like anodic peak (A_2) in between 0.161 and 0.444 V versus SCE, (ii) the onset of an oxidation wave at ~ 0.578 V versus SCE and (iii) a broad reduction peak (C) at ~ −0.544 V versus SCE. This cyclic voltammogram exhibits good resemblance with the tenth potential sweep [cf., Fig. 2(a)] recorded during the synthesis of PANI layer on LCS electrode. The oxidation wave is attributed to oxidation of aniline and it is found that an onset of the oxidation wave (indicated by an arrow) occurs at lower potential (0.696 V vs. SCE) than one observed with an uncoated LCS. This indicates that electropolymerization of PANI layer is mediated by the previously deposited POA layer on LCS leading to the bi-layer structure. The current densities corresponding to the redox peaks are comparable to those observed with an uncoated LCS electrode, indicating that the rate of polymerization of aniline is unaffected on an electrode already covered with a POA.

During second sweep, the voltammogram identical to that of first sweep is obtained except an increase in the current densities corresponding to the redox peaks. After third sweep, the current densities corresponding to the anodic peaks decrease gradually with an increase in the number of sweeps. A typical 10th sweep is also shown in Figure 2(d). The thickness of bi-layered PANI/POA composite calculated by using the eq. (1) was found to be ~ 9.66 μm (SD = 0.10).

The FTIR spectrum of PANI/POA coating on LCS [Fig. 3(d)] recorded in HATR mode exhibits main characteristic bands due to PANI which indicates that the electrochemical polymerization of aniline takes place on POA layer and results into the formation of bi-layered PANI/POA composite on the LCS.

The SEM micrographs of PANI/LCS, POA/LCS, POA/PANI/LCS and PANI/POA/LCS are shown in Figure 4. The surface morphology of the single layers as well as bi-layered composites is relatively uniform, crack free, and featureless.

Evaluation of corrosion protection performance

The corrosion protection performance of PANI, POA and bi-layered composites POA/PANI and PANI/POA was evaluated in 3% NaCl solution by using OCP measurements, potentiodynamic polarization technique and EIS.

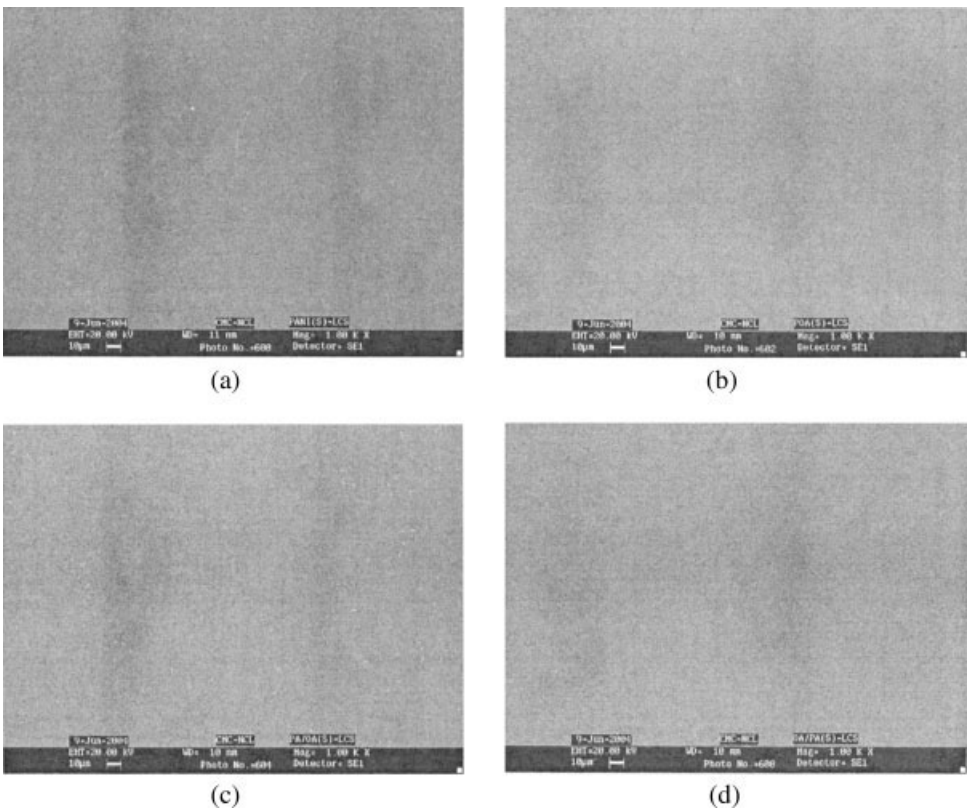

Figure 4 SEM micrographs of (a) PANI, (b) POA, (c) POA/PANI, and (d) PANI/POA coatings synthesized on LCS substrate.

OCP measurements

The evolution of OCP for PANI/LCS, POA/LCS, POA/PANI/LCS and PANI/POA/LCS as a function of immersion time in 3% NaCl was studied. The corresponding OCP-time curves are depicted in Figure 5. Initially, the OCP of PANI/LCS [Fig. 5(a)] was measured to be ~ -0.483 V versus SCE, which is more positive than that of the uncoated LCS by up to ~ 0.227 V versus SCE. The initial decrease in the potential is associated with the initiation of the water uptake process in the coating. After 8 h of immersion the potential decreases sharply and it remains fairly constant at ~ -0.608 V versus SCE, which is close to the corrosion potential of LCS. The protection time of the coating is determined by measuring the elapsed time until the OCP of the polymer coated LCS drops to that of the uncoated electrode. Thus, the PANI protects the LCS in 3% NaCl for almost 8 h.

On the other hand, the OCP value of POA/LCS [Fig. 5(b)] was measured to be ~ -0.440 V versus SCE and it is more positive than that of the uncoated LCS by up to ~ 0.270 V versus SCE. In the early stages of the immersion, the potential decreases sharply and it attains a plateau wherein the potential remains fairly constant at ~ -0.553 V versus SCE during the first 5 h of immersion. This plateau is observed for 24 h during which the POA coating exhibits barrier behavior by limiting the diffusion of the corrosive species towards the underlying steel substrate. After 24 h of immersion, the potential decreases to -0.612 V versus SCE, that is close to the corrosion potential of the uncoated LCS.

The OCP-time curves recorded for LCS coated with bi-layered POA/PANI and PANI/POA composites are presented in Figure 5(c,d), respectively. The OCP curves for bi-layered composites exhibit behavior that is somewhat similar to those of the single layers. However, a significant improvement in the protection time is observed. Initially, the POA/PANI/LCS and PANI/POA/LCS exhibit the OCP values of -0.465 and -0.433 V versus SCE, respectively. Both the potential values are more positive than that of the uncoated LCS under the same experimental conditions.

In the case of POA/PANI/LCS [Fig. 5(c)], initially the potential decreases and it attains a plateau wherein the potential remains fairly constant at ~ -0.536 V versus SCE during the first 11 h of immersion. This plateau is observed for 169 h during which the potential remains fairly constant at ~ -0.536 V versus SCE. After about 169 h the LCS is no longer protected by bi-layer POA/PANI and potential drops to the corrosion potential of the substrate.

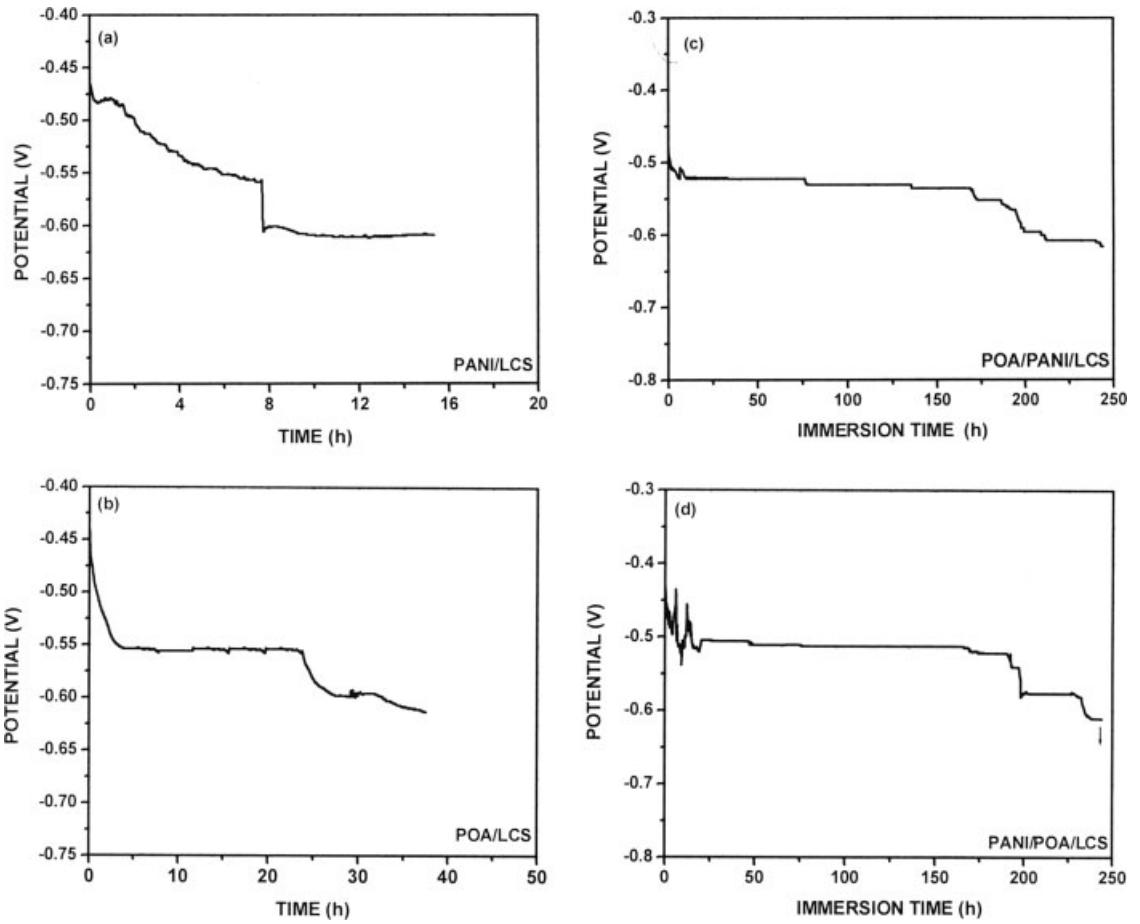

Figure 5 OCP-time curves recorded for (a) PANI/LCS, (b) POA/LCS, (c) POA/PANI/LCS, and (d) PANI/POA/LCS in aqueous 3% NaCl.

On the other hand, in the case of PANI/POA/LCS [Fig. 5(d)], the OCP decreases during the early stages of the immersion and after first 22 h of immersion, a nearly constant potential plateau is reached. This first plateau is observed for 193 h during which the OCP remains fairly constant at ~ -0.505 V versus SCE. After about 193 h, the potential decreases sharply and a second plateau is seen around -0.580 V versus SCE, which is still more positive than that of the uncoated LCS. The duration of the second plateau is shorter ($\sim$ 38 h) and finally, after 230 h the potential decreases sharply to -0.611 V versus SCE, which is close to the corrosion potential of the LCS. Thus, the bi-layered PANI/POA composite protects the LCS in 3% NaCl for almost 230 h.

Potentiodynamic polarization measurements

The potentiodynamic polarization curves recorded in 3% NaCl for an uncoated LCS, PANI/LCS, POA/LCS, POA/PANI/LCS, and PANI/POA/LCS are shown in Figure 6. The values of the E_{corr}, j_{corr}, Tafel constants (β_a and β_c), polarization resistance (R_{pol}) and CR obtained from these curves are given in Table I. The mean value and SD of CR are also given in Table I. The positive shifts in the E_{corr}, as compared to uncoated LCS, were observed for all the

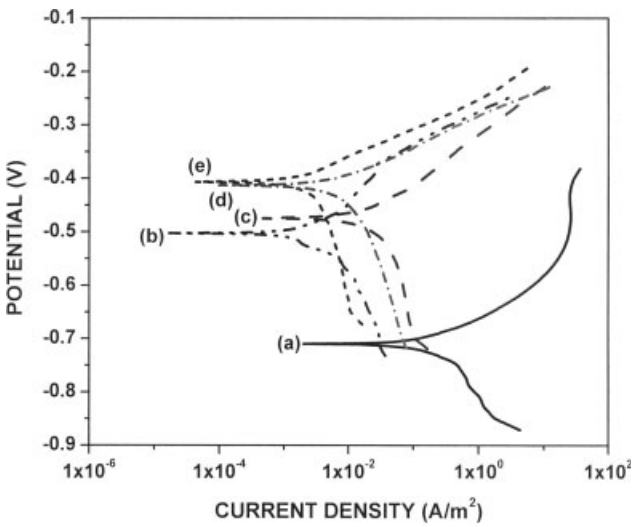

Figure 6 Potentiodynamic polarization curves for (a) uncoated LCS, (b) PANI/LCS, (c) POA/LCS, (d) POA/PANI/LCS, and (e) PANI/POA/LCS recorded in aqueous 3% NaCl solution.

TABLE I
Potentiodynamic Polarization Measurement Results

Sample	E_{corr} (V)	I_{corr} (A/m^2)	β_a V/dec	β_c V/dec	R_p Ω/m^2	CR (mm/yr) (mean value, SD)	% P
Bare LCS	−0.710	0.3071	0.084	0.185	8.22×10^2	0.35 (0.3466, 4.22×10^{-4})	—
PANI coated LCS (~2.90 μm thick, SD = 0.085)	−0.502	0.0096	0.225	0.399	6.51×10^4	0.01 (0.012, 2.10×10^{-3})	2.00×10^{-3}
POA coated LCS (~6 μm thick, SD = 0.081)	−0.474	0.0361	0.112	0.396	1.05×10^4	0.04 (0.0416, 2.40×10^{-3})	1.20×10^{-2}
POA/PANI coated LCS (~6 μm thick, SD = 0.081)	−0.414	0.0067	0.061	0.180	2.97×10^4	0.008 (0.0073, 3.3×10^{-4})	8.70×10^{-4}
PANI/POA coated LCS (~9.66 μm thick, SD = 0.10)	−0.406	0.0031	0.065	0.369	2.85×10^5	0.004 (0.0039, 4.6×10^{-4})	7.34×10^{-5}

conducting polymer coatings. The shift in the E_{corr} depends on type of the coating and it decreases in the order PANI/POA > POA/PANI > POA > PANI. The decrease in the j_{corr} for uncoated LCS was observed from 0.3071 A/m^2 to 0.0096, 0.036, 0.0067, and 0.0031 A/m^2 for PANI, POA, POA/PANI and PANI/POA coatings, respectively. The CRs of PANI, POA, POA/PANI, and PANI/POA coated LCS are found to be ~ 0.01, 0.04, 0.008, and 0.004 mm/year, which are ~ 35, 9, 44, and 88 times lower than that observed for uncoated LCS. Thus, the corrosion protection offered to LCS by bi-layered composite coatings of PANI and POA is dependent on the order in which the coatings were deposited. The PANI/POA coating provides better protection to LCS against corrosion than POA/PANI coating. Nevertheless, both combinations of the bi-layered composite coatings, i.e., POA/PANI and PANI/POA provide effective protection to LCS than a single layered PANI and POA coatings.

The porosity in the coating is very important parameter which decides its suitability to protect the substrate against corrosion. To calculate the porosity of these deposits, we have used the relationship[47]:

$$P = \frac{R_{pol}(\text{uncoated})}{R_{pol}(\text{coated})} 10^{-\left(\frac{\Delta E_{corr}}{\beta_a}\right)} \quad (2)$$

where P is the total porosity, R_{pol} (uncoated) is the polarization resistance of uncoated LCS, R_{pol} (coated) is the measured polarization resistance for coated LCS, ΔE_{corr} is the difference between corrosion potentials and β_a the anodic Tafel slope for uncoated LCS substrate. Table I also gives the porosity values in the polymer deposits. The porosity in polymer coatings depends on the type of the coating and it decreases in the order PANI > POA > POA/PANI > PANI/POA. Thus, PANI/POA coating is more compact than other coatings and the porosity in this bi-layered composite is almost 12, 27, and 163 times lower than porosity in POA/PANI, PANI, and POA coatings.

EIS studies

The Nyquist impedance plots of uncoated LCS, PANI/LCS, POA/LCS, POA/PANI/LCS, and PANI/POA/LCS recorded in 3% NaCl are shown in Figure 7. The Nyquist impedance plot of uncoated LCS [Fig. 7(a)] is modeled by an electrical equivalent circuit depicted in the Figure 8(a), where R_s represents the electrolyte resistance, CPE_p the phase element that represents all the frequency dependent electrochemical phenomena, namely double layer capacitance (C_{dl}) and diffusion processes and R_{ct} the charge transfer resistance connected with corrosion processes. The constant phase element, CPE, is introduced in the circuit instead of a pure capacitor to give a more accurate fit. Thus, the impedance plot of the uncoated LCS can be fitted with a semicircle, which is attributed to the processes occurring at the steel surface.

The Nyquist impedance plots of PANI/LCS [Fig. 7(b)], POA/LCS [Fig. 7(c)], POA/PANI/LCS [Fig. 7(d)], and PANI/POA/LCS [Fig. 7(e)] were modeled by the electrical equivalent circuit, model B, shown in the Figure 8(b). It consists of R_s, constant phase element CPE_c connected with coating capacitance, pore resistance R_p, CPE_p and R_{ct} connected with corrosion processes in the bottom of the pores. Thus, these impedance plots were fitted with two semicircles, a smaller one at high frequency range followed by a larger one at lower frequencies. The first semicircle is attributed to the characteristics of the polymer/electrolyte interface and it is characterized by R_p and CPE_c.[7,9,14,48] The second semicircle in the low frequency region is attributed to the polymer/LCS interface and it is characterized by R_{ct} for the charge transfer reactions occurring at the bottom of the pores in the coating and CPE_p.[7,9,14,48] The values of the impedance parameters of the best fit to the experimental impedance plots for uncoated LCS and polymer coated LCS are given in Table II. The values of R_{ct} for PANI/LCS, POA/LCS, POA/PANI/LCS and PANI/POA/LCS are found to be ~ 12.345, 4.562, 10.531, and 23.356 kΩ, respectively, which are

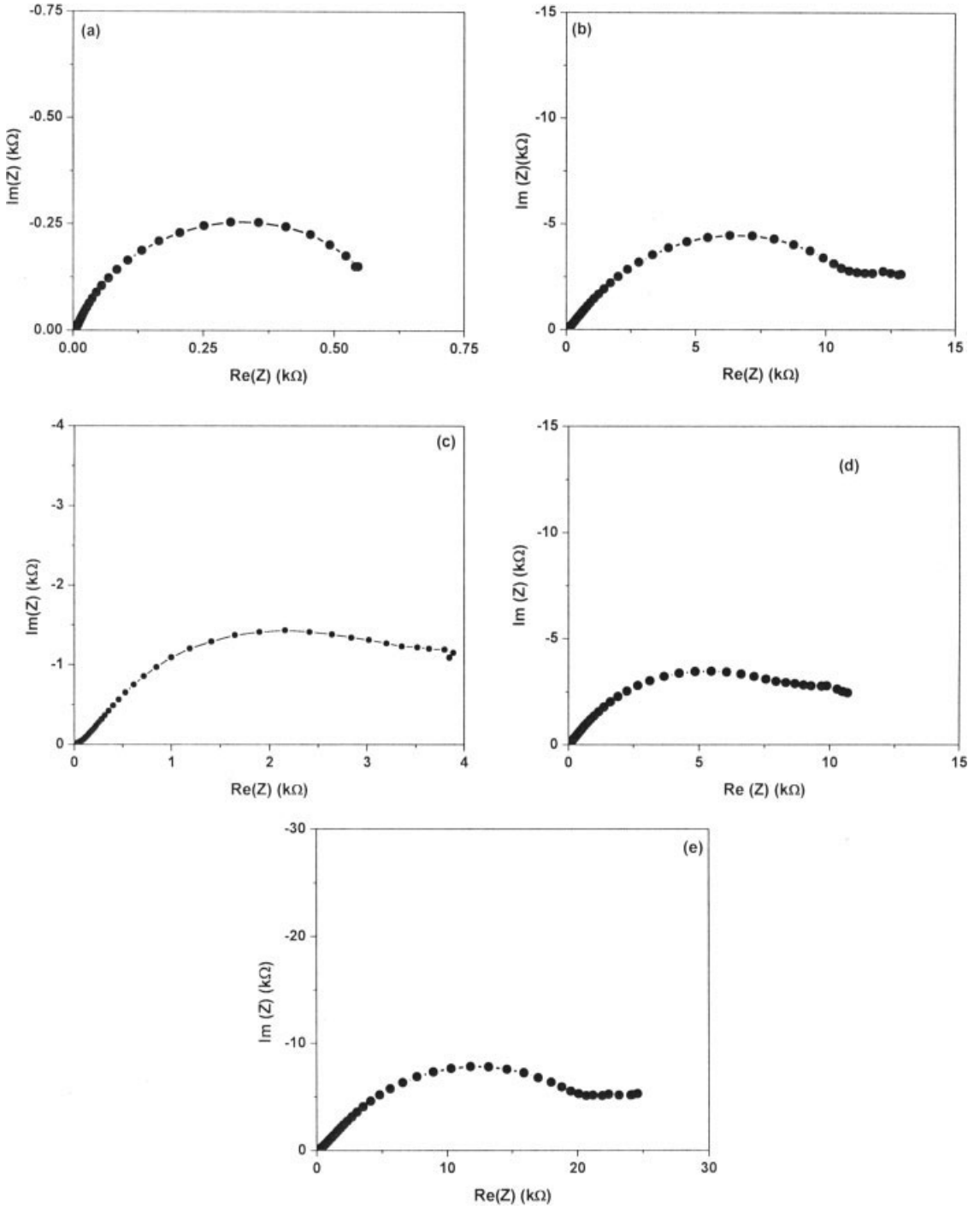

Figure 7 Nyquist impedance plots of (a) uncoated LCS, (b) PANI/LCS, (c) POA/LCS, (d) POA/PANI/LCS, and (e) PANI/POA/LCS recorded in aqueous 3% NaCl solution.

about ~ 19, 7, 16, and 36 times higher than that observed for uncoated LCS. The protective effect of PANI, POA, POA/PANI, and PANI/POA is obvious as the R_{ct} values are significantly higher as compared to the uncoated LCS.[49] However, bi-layered PANI/POA composite provides effective protection to LCS against corrosion than PANI, POA, and POA/PANI, which is in agreement with the potentiodynamic polarization results.

Immersion tests

To gain further insight into corrosion protection properties of the PANI, POA, POA/PANI, and

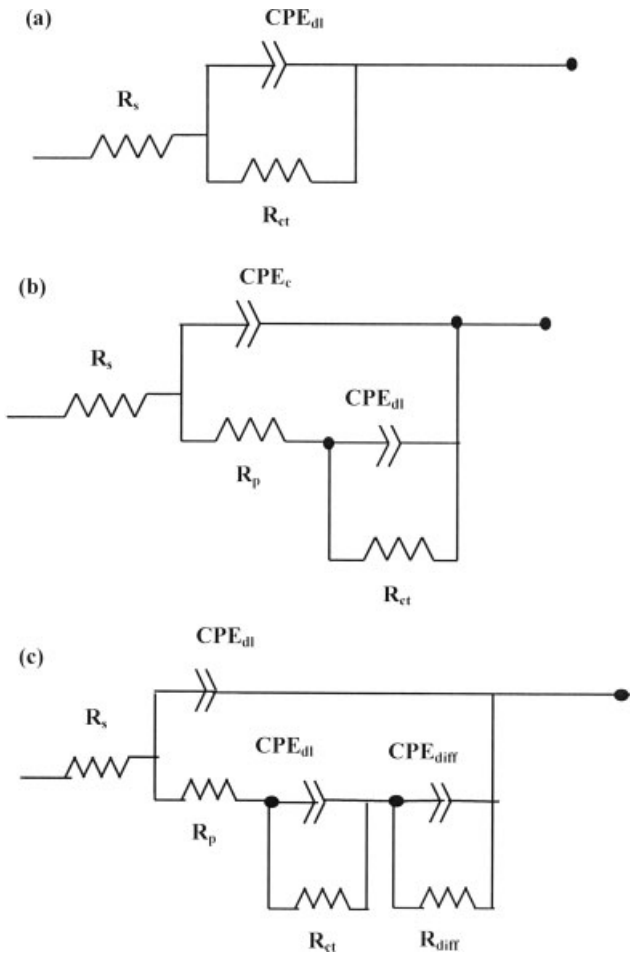

Figure 8 Electrical equivalent circuit models (a) model A, (b) model B, and (c) model C used for the fitting of impedance plots.

PANI/POA coatings, the impedance plots were recorded as a function of immersion time in 3% NaCl solution. The Nyquist impedance plots of PANI/LCS recorded after 2, 4, and 16 h of immersion times in aqueous 3% NaCl are shown in Figure 9. These impedance plots exhibit systematic variations in terms of the values of the impedance parameters, which are the result of the changes in the dielectric characteristics of the coating because of electrolyte penetration through the pores in the coating and consequently, the onset of corrosive processes at the surface of the LCS substrate.

The Nyquist impedance plots recorded after 2 and 4 h of immersion times [Fig. 9(a,b)] were analyzed in terms of the same equivalent circuit model A, as shown in the Figure 8(b). These plots are fitted with two semicircles with diameters R_p (at higher frequency range) and R_{ct} (at lower frequencies).

The R_{ct} value is observed to increase, whereas the R_p decreases after 2 h of immersion time. The decrease in R_p value is attributed to the entry of the electrolyte into the micropores in the coating.[50] While an increase in R_{ct} value is attributed to the oxidation of the LCS by the conducting polymer, which results into the formation of iron oxide compounds at the PANI/LCS interface and also to partial reduction of the polymer film.

The R_{ct} value is observed to increase further, whereas the R_p decreases further after 4 h of immersion time. The increase in the R_{ct} value may be attributed to the further reduction of the polymer film and formation of the thicker layer of the protective iron oxide compounds. The E_{corr} value at this immersion time is measured to be -0.510 V versus SCE, which is more positive than that of the corrosion potential for the uncoated mild steel by upto 0.200 V. Therefore, it can be said that during first 4 h of immersion, the detectable corrosion processes were not started at the LCS substrate surface under the coating.

The Nyquist impedance plot of the PANI/LCS recorded after 16 h of immersion time in 3% NaCl solution [Fig. 9(c)] cannot be well fitted to model A. During immersion, the electrolyte penetrates via the pores in the coating and develops the electrolyte pathways with time through coating. The corrosive species along with the water diffuse through these paths towards the steel surface. When the sufficient amount of electrolyte reaches to the LCS surface, the corrosion processes are initiated at the POA/LCS interface and as a consequence the E_{corr} value shifts to less noble value. The measured open circuit potential value at this moment is found to be ~ -0.550 V versus SCE. Therefore, it can be said that after 16 h of immersion the anodic dissolution of the passive oxide layer begins at the bottom of the pores which interacts with the electrolyte solution and results into the formation of corrosion products which diffuse towards the coating surface through the pores in the coating.

More recently, we have investigated the corrosion protection performance of POA coatings on LCS in 3% NaCl through immersion tests by EIS.[51] It was observed that a single equivalent circuit was inadequate to explain the various physical and electrochemical processes occurring at different immersion times. It was shown that a diffusion combination, which consists of the diffusion resistance (R_{diff}) and the diffusion capacitance (C_{diff}) related to the diffusion of corrosion products from steel surface towards coating must be considered in the equivalent circuit after a certain immersion time. The same equivalent circuit, model C, depicted in the Figure 8(c) was used to fit the impedance plot of PANI/LCS recorded after 16 h of immersion. The model C consists of three time constants in which the first time constant is a representative of the characteristics of the PANI coating, while the second and third capacitive loops are attributed to the complex reac-

TABLE II
Impedance Parameter Values Extracted from the Fit to the Equivalent Circuit for the Impedance Spectra Recorded in Aqueous 3% NaCl Solution

Immersion time	R_p (ohm)	C_c (F/m)	R_{ct} (ohm)	C_{dl} (F/m)	R_{diff} (ohm)	C_{diff} (F/m)
Uncoated LCS						
As it is	—	—	6.54×10^{2}	7.99×10^{-4}	—	—
PANI coated LCS						
As it is	1483	1.10×10^{-5}	12.35×10^{3}	1.67×10^{-6}	—	—
2 h	732	1.63×10^{-5}	18.98×10^{3}	1.09×10^{-6}	—	—
4 h	403	3.64×10^{-5}	19.19×10^{3}	3.02×10^{-6}		
16 h	68.94	7.36×10^{-5}	11.26×10^{2}	4.70×10^{-5}	47.36×10^{2}	1.42×10^{-5}
POA coated LCS						
As it is	125	1.83×10^{-5}	45.62×10^{2}	5.31×10^{-5}	—	—
2 h	275	3.95×10^{-5}	55.36×10^{2}	1.19×10^{-5}	—	—
4 h	250	4.09×10^{-5}	74.90×10^{2}	1.48×10^{-5}	—	—
16 h	58	1.44×10^{-4}	55.39×10^{2}	5.21×10^{-5}	35.26×10^{2}	3.75×10^{-4}
48 h	50	1.54×10^{-4}	48.73×10^{2}	5.70×10^{-5}	51.32×10^{2}	1.97×10^{-4}
72 h	40	2.05×10^{-4}	31.99×10^{2}	4.09×10^{-4}	61.63×10^{2}	2.24×10^{-4}
POA/PANI coated LCS						
As it is	995	1.51×10^{-5}	10.53×10^{3}	2.22×10^{-6}	—	—
2 h	900	1.76×10^{-5}	16.36×10^{3}	4.79×10^{-6}	—	—
4 h	899	2.53×10^{-5}	26.97×10^{3}	6.57×10^{-6}	—	—
16 h	700	2.66×10^{-5}	15.10×10^{3}	3.30×10^{-5}	—	—
48 h	500	3.89×10^{-5}	35.09×10^{2}	3.36×10^{-5}	—	—
72 h	494	4.46×10^{-5}	35.00×10^{2}	3.53×10^{-5}	26.57×10^{2}	3.52×10^{-4}
96 h	250	8.93×10^{-5}	15.00×10^{2}	4.58×10^{-5}	32.93×10^{2}	3.71×10^{-4}
120 h	240	9.17×10^{-5}	91.20×10^{1}	6.92×10^{-5}	36.48×10^{2}	9.62×10^{-4}
240 h	200	1.72×10^{-4}	90.00×10^{1}	5.80×10^{-4}	52.89×10^{2}	1.26×10^{-3}
PANI/POA coated LCS						
As it is	1589	3.44×10^{-6}	23.36×10^{3}	2.47×10^{-6}	—	—
2 h	1580	3.66×10^{-6}	23.57×10^{3}	7.65×10^{-6}	—	—
4 h	1431	3.86×10^{-6}	23.75×10^{3}	7.76×10^{-6}	—	—
16 h	1400	3.99×10^{-6}	50.50×10^{3}	7.80×10^{-6}	—	—
48 h	1000	4.26×10^{-6}	45.89×10^{3}	8.99×10^{-6}	72.00×10^{5}	1.31×10^{-4}
72 h	1000	4.66×10^{-6}	42.25×10^{3}	1.16×10^{-5}	75.44×10^{5}	1.14×10^{-4}
96 h	1000	4.75×10^{-6}	40.57×10^{2}	1.56×10^{-5}	82.79×10^{3}	6.01×10^{-5}
120 h	800	5.43×10^{-6}	37.45×10^{2}	1.89×10^{-5}	89.27×10^{3}	5.65×10^{-5}
240 h	725	5.57×10^{-6}	35.42×10^{2}	1.95×10^{-5}	16.25×10^{3}	8.62×10^{-6}

tions occurring at the surface of the LCS substrate. The second loop is characterized by charge transfer resistance (R_{ct}) and double layer capacitance (C_{dl}) and the third loop is correlated to diffusion processes (R_{diff} and C_{diff}) caused by presence of corrosion products. It is found that the fitting curve gives a good fit to the experimental impedance plot after 16 h of immersion when the equivalent circuit model C is used.

After 16 h of immersion, the R_{ct} value is observed to decrease and its value is found to be $\sim$ 1.126 kΩ. However, it is higher than that of the uncoated LCS. The decrease in the value of R_{ct} may be due to the dissolution of the passive oxide layer on the LCS surface. The diffusion resistance is the resistance against the diffusion of the corrosion products from LCS surface towards coating and its value is observed to be 4.736 kΩ.

After 48 h of immersion, the detachment of the coating was observed, when the working electrode was removed from the test electrolyte and therefore, the immersion study was terminated at the end of the 16 h.

The Nyquist impedance plots of POA/LCS, POA/PANI/LCS, and PANI/POA/LCS recorded for various immersion times in aqueous 3% NaCl solution are presented in Figures S1–S3 (see supplementary material at http://www.interscience.wiley.com/jpages/0021-8995/suppmat.).

Evolution of impedance parameters with immersion time

The variation of R_p for PANI/LCS, POA/LCS, POA/PANI/LCS, and PANI/POA/LCS as a function of immersion time is shown in Figure 10(a). It is seen that the value of R_p decreases rapidly and the most for PANI/LCS and POA/LCS. Moreover, even after 240 h of immersion, the values of R_p for both combinations of bi-layered composites are found to be higher than those observed for PANI and POA after 16 and 72 h of immersion, respectively. In the

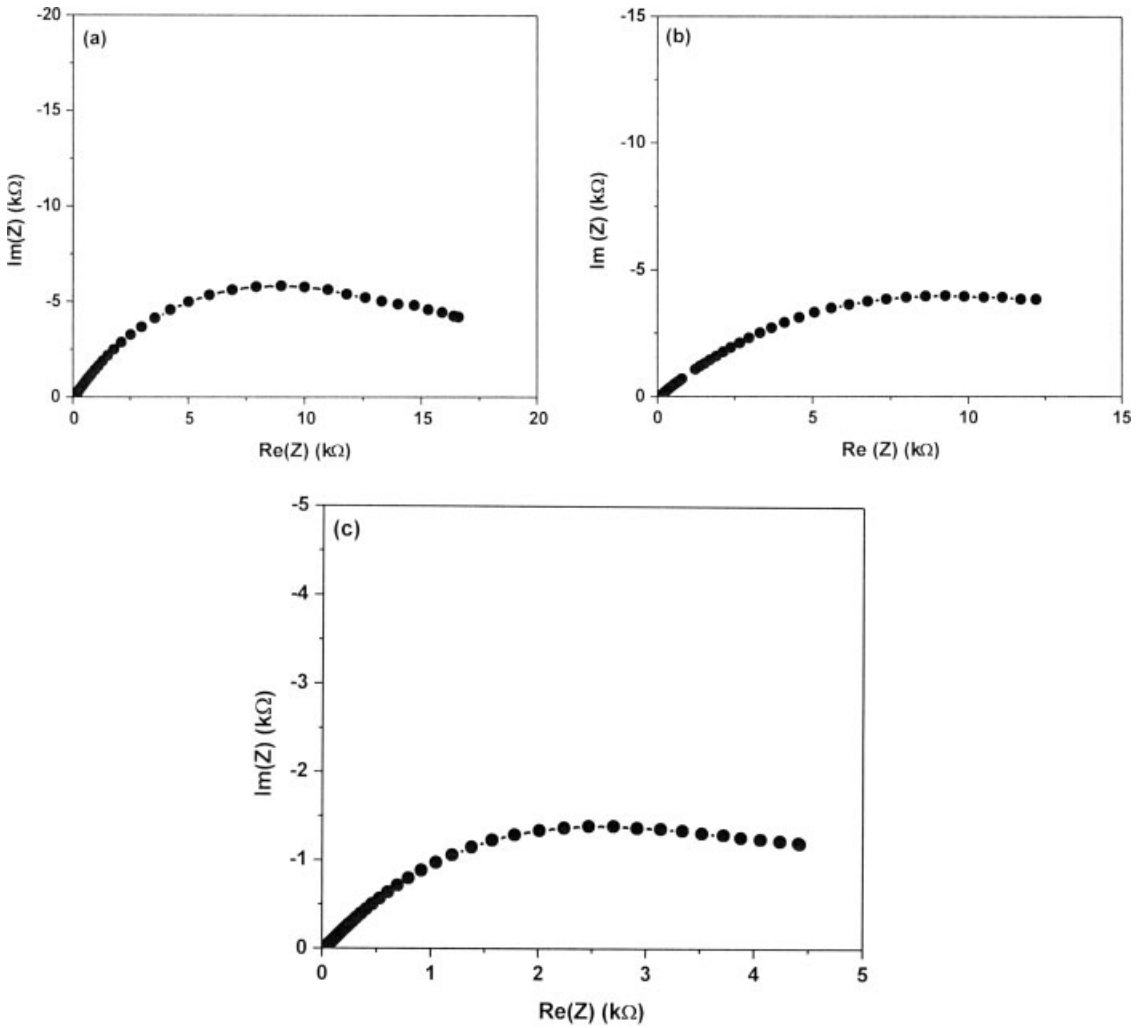

Figure 9 Nyquist impedance plots for PANI/LCS recorded after (a) 2, (b) 4, and (c) 16 h of immersion in 3% NaCl.

case of PANI/LCS, a rapid and continuous decrease in the value of R_p reveals that single layered PANI coating provides the least corrosion protection. A slow decrease in the value of R_p is observed for the bi-layered POA/PANI composite. Almost constant value of R_p for PANI/POA composite denotes that development of electrolyte pathways through the composite reached to steady state since the first measurements.

The coating capacitance C_c is the capacitance of the intact coating layer or the capacitance of the areas where rapid solution uptake does not occur.[50] The evolution of the C_c with the immersion time is shown in Figure 10(b). The increase in the values of C_c for PANI, POA, and POA/PANI can be interpreted as consequence of continuous water uptake. The values of C_c for the bi-layered PANI/POA composite are significantly lower than those observed for PANI, POA, and POA/PANI even after 240 h of immersion. Further more, the values of C_c remains fairly constant for PANI/POA composite which reveals that water permeation is very small up to 240 h of immersion.

The volume fraction of the water in the polymer coating when in contact with 3% NaCl solution as a function of time is determined using Brasher–Kingsbury equation[52]

$$\phi = \frac{\log C_t / C_o}{\log 80} \tag{3}$$

where C_t is the coating capacitance at an instant t and C_o the capacitance at time $t = 0$; the value 80 is the dielectric constant of water at 25°C. The volume fraction of water in the coating as a function of immersion time is shown in Figure 10(c). It is seen that water permeation in the bi-layered PANI/POA composite is very small up to 240 h of immersion, which shows that this composite resists water uptake and it is corrosion resistant.

The variation of R_{ct} as a function of the immersion time is shown in Figure 10(d). It is observed that for

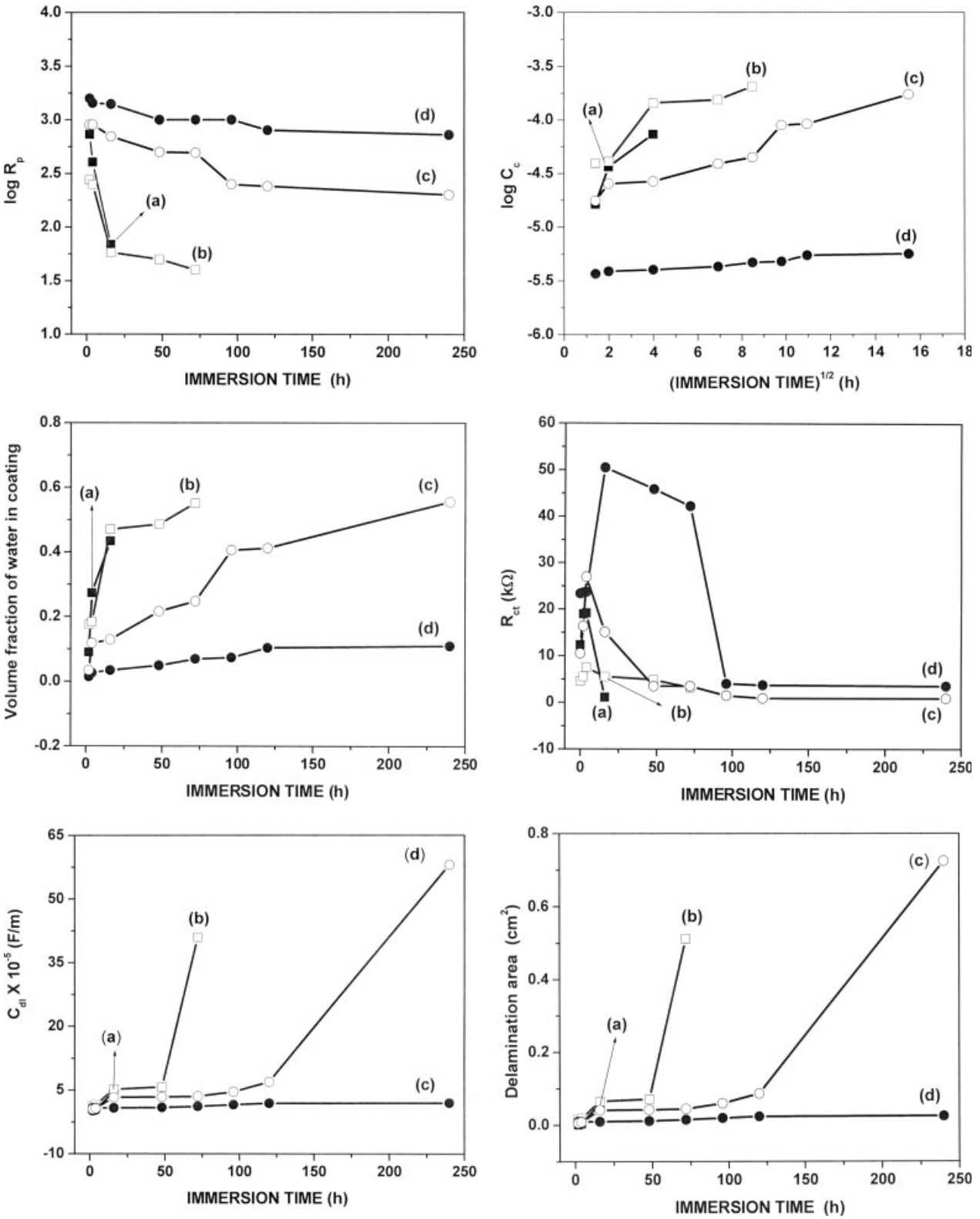

Figure 10 (a) : Variation of pore resistance (R_p) for (a) PANI/LCS, (b) POA/LCS, (c) POA/PANI/LCS, and (d) PANI/POA/LCS with immersion time in 3% NaCl. (b) Variation of coating capacitance (C_c) for (a) PANI/LCS, (b) POA/LCS, (c) POA/PANI/LCS, and (d) PANI/POA/LCS with immersion time in 3% NaCl. (c) Volume fraction of the electrolyte in (a) PANI, (b) POA, (c) POA/PANI, and (d) PANI/POA coating as a function of immersion time in 3% NaCl. (d) Variation of charge transfer resistance (R_{ct}) for (a) PANI/LCS, (b) POA/LCS, (c) POA/PANI/LCS, and (d) PANI/POA/LCS with immersion time in 3% NaCl. (e) Variation of double layer capacitance (C_{dl}) for (a) PANI/LCS, (b) POA/LCS, (c) POA/PANI/LCS and (d) PANI/POA/LCS with immersion time in 3% NaCl. (f) Delamination area for (a) PANI/LCS, (b) POA/LCS, (c) POA/PANI/LCS, and (d) PANI/POA/LCS as a function of immersion time in 3% NaCl.

PANI, POA, POA/PANI, and PANI/POA coatings, the R_{ct} value increases up to 2, 4, 4 and 16 h of immersion, respectively, and thereafter it decreases with the immersion time, however, it is higher than the uncoated LCS. The increase in the R_{ct} value is attributed to the formation of protective oxide layers and the effective barrier behavior of the coating. The decrease in the R_{ct} value with an increase in the immersion time reveals an initiation of the corrosion processes. The PANI coating provides the least corrosion protection followed by POA and POA/PANI coatings. In the case of PANI/POA composite, the corrosion processes begins after the 48 h of immersion and after 240 h of immersion the R_{ct} value is found to be $\sim$ 3.542 kΩ which is about $\sim$ 5 times higher than that observed for uncoated LCS. Thus, the PANI/POA coating provides better protection to LCS against corrosion than PANI, POA, POA/PANI coatings.

The double layer capacitance C_{dl} represents the wet area under the coating, which is the area in contact with the electrolyte. The value of C_{dl} for PANI, POA and bi-layered composite POA/PANI [Fig. 10(e)] increases sharply after 4, 48, and 120 h of immersion, respectively, which indicates an increase in the area at which delamination and/or corrosion occurred under the coating. It is observed that for PANI/POA composite C_{dl} value is the lowest and it remains almost constant up to immersion time of 240 h indicating that this bi-layered composite provides better protection to LCS than PANI, POA, and POA/PANI composite.

The delamination area is evaluated by comparing the values of the measured C_{dl} with a specific capacitance C_{dl} (measured on uncoated substrate).[53] The determined delamination area values as a function of immersion time [Fig. 10(f)] clearly indicates negligible delamination up to 240 h as evident from the lowest values of the order of 0.009–0.0245 cm^2. This confirms the stability of PANI/POA composite coating on LCS when exposed to 3% NaCl solution.

CONCLUSIONS

Bi-layered composites of PANI and POA were successfully synthesized on LCS from an aqueous salicylate solution by using cyclic voltammetry. The single layer of PANI and POA protected the LCS in 3% NaCl for 8 and 16 h, respectively. Both combinations of the bi-layered composite coatings, i.e., POA/PANI (POA on top of the PANI) and PANI/POA (PANI on top of the POA) provided effective protection to LCS than a single layered PANI or POA coating. However, the corrosion protection offered to LCS depends on the deposition order of polymer layers in the composite. The PANI/POA composite provides better protection to LCS against corrosion than POA/PANI coating. The CRs of PANI, POA, POA/PANI, and PANI/POA coated LCS are found to be $\sim$ 0.01, 0.04, 0.008, and 0.004 mm/year, which are $\sim$ 35, 9, 44, and 88 times lower than that observed for uncoated LCS. The bi-layered composites prevented corrosion of the steel for longer time.

References

1. Skotheim, T. A.; Reynolds, J. R., Eds. Handbook of Conducting Polymers, Vols. I and II, 3rd ed.; CRC Press, Taylor and Francis Group: New York, 2007.
2. Bazzaoui, M.; Martins, J. I.; Costa, S. C.; Bazzaoui, E. A.; Reis, T. C.; Martins, L. Electrochim Acta 2006, 51, 2417.
3. Bazzaoui, M.; Martins, J. I.; Costa, S. C.; Bazzaoui, E. A.; Reis, T. C.; Martins, L. Electrochim Acta 2006, 51, 4516.
4. Yagan, A.; Ozcicek Pekmez, N.; Yıldız, A. Electrochim Acta 2006, 51, 2949.
5. Popovic, M. M.; Grgur, B. N. Synth Met 2004, 143, 191.
6. Moraes, S. R.; Vilca, D. H.; Motheo, A. J. Prog Org Coat 2003, 48, 28.
7. Fenelon, A. M.; Breslin, C. B. Electrochim Acta 2002, 47, 4467.
8. Sazou, D.; Synth Met 2001, 118, 133.
9. Su, W.; Iroh, J. O. Synth Met 2000, 114, 225.
10. Bernard, M. C.; Hugot-Le Goff, A.; Joireta, S.; Dinh, N. N.; Toanb, N. N. J Electrochem Soc 1999, 146, 995.
11. Chaudhari, S.; Sainkar, S. R.; Patil, P. P. Prog Org Coat 2007, 58, 54.
12. Kraljic, M.; Mandic, Z.; Duic, L. J. Corros Sci 2003, 45, 181.
13. Paliwoda-Porebska, G.; Stratmann, M.; Rohwerder, M.; Potje-Kamloth, K.; Lu, Y.; Pich, A. Z.; Adler, H.-J. Corros Sci 2005, 47, 3216.
14. Fenelon, A. M.; Breslin, C. B. Surf Coat Technol 2005, 190, 264.
15. Sazou, D. Synth Met 2001, 118, 133.
16. Patil, S.; Sainkar, S. R.; Patil, P. P. Appl Surf Sci 2004, 225, 204.
17. Shinde, V.; Sainkar, S. R.; Patil, P. P. Corros Sci 2005, 47, 1352.
18. Chaudhari, S.; Sainkar, S. R.; Patil, P. P. J Phys D: Appl Phys 2007, 40, 520.
19. Ogurtsov, N. A.; Pud, A. A.; Kamarchik, P.; Shapoval, G. Synth Met 2004, 143, 43.
20. Shah, K.; Iroh, J. Synth Met 2002, 132, 35.
21. Breslin, C. B.; Fenelon, A. M.; Conroy, K. G.; Mater Des 2005, 26, 233.
22. Ogurtsov, N. A.; Shapoval, G. S. Russ J Appl Chem 2006, 79, 605.
23. Grgur, B. N.; Zivkovic, P.; Gvozdenovic, M. M. Prog Org Coat 2006, 56, 240.
24. Wankhede, M. G.; Gaikwad, A. B.; Patil, P. P. Surf Coat Technol 2006, 201, 2240.
25. Bazzaoui, M.; Martins, J. I.; Bazzaoui, E. A.; Reis, T. C.; Martins, L. J Appl Electrochem 2004, 34, 815.
26. Wankhede, M. G.; Gangal, S. A.; Patil, P. P. Corros Eng Sci Technol 2005, 40, 121.
27. Martins, J. I.; Bazzaoui, M.; Reis, T. C.; Bazzaoui, E. A.; Martins, L. I. Synth Met 2002, 129, 221.
28. Pawar, P.; Sainkar, S. R.; Patil, P. P. J Appl Polym Sci 2007, 103, 1868.
29. Hur, E.; Bereket, G.; Sahin, Y. Prog Org Coat 2005, 54, 63.
30. Bereket, G.; Hur, E.; Sahin, Y. Curr Appl Phys 2007, 7, 597.
31. Pawar, P.; Gaikwad, A. B.; Patil, P. P. Electrochim Acta 2007, 52, 5958.
32. Yagan, A.; Ozcicek Pekmez, N.; Yıldız, A. Prog Org Coat 2007, 59, 297.
33. Tuken, T.; Ozyilmaz, A. T.; Yazici, B.; Kardas, G.; Erbil, M. Prog Org Coat 2004, 51, 27.

34. Ozyilmaz, A. T.; Kardas, G.; Erbil, M. Yazici, B. Appl Surf Sci 2005, 242, 97.
35. Tuken, T.; Ozyilmaz, A. T.; Yazici, B.; Erbil, M. Appl Surf Sci 2004, 236, 292.
36. Tuken, T.; Yazici, B.; Erbil, M. Prog Org Coat 2004, 50, 115.
37. Chaudhari, S.; Mandale, A. B.; Patil K. R.; Sainkar, S. R.; Patil, P. P. J Appl Polym Sci 2007, 106, 220.
38. Electrochemical Corrosion software—CorrWare and CorrView. Electrochemical Corrosion software—CorrWare and CorrView. Scribner Associates: Southern Pines, NC.
39. Electrochemical impedance software—Z-plot and Z-view. Electrochemical impedance software—Z-plot and Z-view. Scribner Associates: Southern Pines, NC.
40. Pawar, P.; Gaikwad, A. B.; Patil, P. P. Sci Technol Adv Mater 2006, 7, 732.
41. Stillwell, D. E.; Park, S. M. J Electrochem Soc 1988, 135, 2254.
42. Ocon, P.; Cristobal, A. B.; Herrasti, P.; Fatas, E. Corros Sci 2005, 47, 1352.
43. Tang, J.; Jing, X.; Wang, B.; Wang, F. Synth Met 1988, 24, 231.
44. Ohsaka, T.; Ohnuki, Y.; Oyama, N.; Katagiri, G.; Kamisako, K. J Electroanal Chem 1984, 161, 399.
45. Zheng, W. Y.; Levon, K.; Taka, T.; Laakso, J.; Osterholm, J. E. Polym J 1996, 28, 412.
46. Neoh, K. G.; Kang, E. T.; Tan, K. L. J Phys Chem 1991, 95, 10151.
47. Creus, J.; Mazille, H.; Idrissi, H. Surf Coat Technol 2000, 130, 224.
48. Araujo, W. S.; Margarita, C. P.; Ferreira, M.; Matto, O. R.; Neto, P. Electrochim Acta 2001, 46, 1307.
49. Tallman, D. E.; Pae, Y.; Bierwagen, G. P. Corrosion 2000, 56, 401.
50. Miskovic-Stankovic, V. B.; Drazic, D. M.; Teodorovic, M. J Corros Sci 1995, 37, 241.
51. Chaudhari, S.; Patil, P. P. J Appl Polym Sci 2007, 106, 400.
52. Brasher, D. M.; Kingsbury, A. H. J Appl Chem 1954, 4, 62.
53. Li, X. G.; Haung, M. R.; Duan, W.; Yang, Y. L. Chem Rev 2002, 102, 2925.